of more elaborate wall functions or the introduction of a more advanced turbulence model is needed to properly simulate the flowfield in these situations.

Acknowledgments

This research was partially supported by the Naval Sea System Command AHR Grant N00167-86-K-0019 administered by the Office of Naval Research.

References

[1]Patel, V. C., Nakayama, A., and Damian, R., "Measurements in the Thick Axisymmetric Turbulent Boundary Layer Near the Tail of a Body of Revolution," *Journal of Fluid Mechanics*, Vol. 63, No. 2, 1974, pp. 345-362.

[2]Choi, S. K., and Chen, C. J., "Finite Analytic Numerical Solution of Turbulent Flow Past Axisymmetric Bodies," *Proceedings of the Third International Symposium on Refined Flow Modeling and Turbulence Measurements*, edited by Y. Iwasa, Tokyo, 1988, pp. 121-128.

[3]Muraoka, K., "Calculation of Thick Boundary Layer and Wake of Ships by a Partially Parabolic Method," *Proceedings of the 13th ONR Symposium on Naval Hydrodynamics*, Tokyo, 1980, pp. 601-616.

[4]Patankar, S. V., *Numerical Heat Transfer and Fluid Flow*, McGraw-Hill, New York, 1980.

[5]Huang, T. T., Santelli, N., and Belt, G., "Stern Boundary Layer Flow on Axisymmetric Bodies," *Proceedings of the 12th ONR Symposium on Naval Hydrodynamics*, 1978, pp. 127-157.

[6]Launder, B. E., and Spalding, D. B., "The Numerical Calculation of Turbulent Flows," *Computer Methods in Applied Mechanics and Engineering*, Vol. 3, No. 2, 1974, pp. 269-289.

[7]Chen, C. J., and Choi, S. K., "The Finite Analytic Method and Its Applications—Laminar and Turbulent Flow Past Two Dimensional and Axisymmetric Bodies," Vol. 1, Iowa Inst. of Hydraulic Research, Univ. of Iowa, Iowa City, IA, Rept. 334-I, March 1990.

Flow in the Wake of a Freely Rotatable Cylinder with Splitter Plate

J. M. Cimbala* and S. Garg†
Pennsylvania State University,
University Park, Pennsylvania 16802

Introduction

IT is well known[1,2] that a rigidly mounted splitter plate, placed behind a circular cylinder in crossflow, reduces both the cylinder drag and the strength of the shed vortices. Splitter plates have therefore found practical applications, such as suppression of vibration of pitot-static probes in wind and water tunnels. The present work was motivated by the desire to suppress the vibration of a five-hole probe in a water flow, where the oncoming flow direction can be inclined several degrees from the freestream direction, and is not known a priori. In such a case, it was thought that a freely rather than rigidly mounted splitter plate attached to the probe shaft would adjust itself like a weather vane to the changing flow direction. For long plates this was indeed the case, but for shorter plates an unexpected phenomenon was observed. Namely, rather than aligning itself with the flow direction, the splitter plate was observed to rotate to a stable position off axis (on either side of the wake with equal probability). This behavior was first reported by Cimbala et al.,[3] but no explanation of the behavior was given. Their results are summarized in Fig. 1, where stable splitter plate angle θ is plotted as a function of normalized plate length L/D. This angle was found to be independent of Reynolds number for the range tested, which was $5 \times 10^3 < Re < 2 \times 10^4$. As seen, θ decreases continuously with L/D; by $L/D = 5$ the splitter plate, although free to rotate, remains at $\theta = 0$, i.e., parallel to the flow direction.

Recently Xu et al.[4] performed some numerical experiments in an attempt to explain this behavior. Their results show a critical Reynolds number below which the splitter plate is stable at the line of symmetry and above which a symmetry-breaking bifurcation appears. Above the critical Reynolds number, the separation bubble in the cylinder's wake leads to a nonzero unstable moment about the axis, forcing the splitter plate assembly to rotate to a stable position where the moment is zero. Their calculations show that stable splitter plate angle θ decreases with L/D, which agrees qualitatively with the experiments of Cimbala et al.[3] Unfortunately, the maximum Reynolds number of the calculations was 50, far below that of the experiments, and quantitative comparisons are not possible. Nevertheless, the explanation of Xu et al.[4] is considered adequate even for the high Reynolds number experiments. Namely, the time-averaged mean flow in the separated near wake of the cylinder is similar to the steady separation bubble of low Reynolds numbers and imposes an unstable moment on the splitter plate, causing it to migrate to its stable off-axis position. Reynolds number independence implies that the moment is caused primarily by pressure rather than viscous forces. This has been verified[5] in our laboratory by placing a shroud around the front portion of the cylinder, effectively removing the viscous moment. These data are also included in Fig. 1; the shroud has no effect on θ.

Presented here are smoke-wire visualizations and shedding frequency measurements in the wake of the cylinder/splitter plate body. Comparisons are made between the plain cylinder, the cylinder with a splitter plate rigidly fixed at $\theta = 0$ deg, and the freely rotatable cylinder/splitter plate body.

Results and Discussion

The experiments were conducted in a wind tunnel, using a two-dimensional circular cylinder with a splitter plate attached. The cylinder/splitter plate combination could be made freely rotatable about the longitudinal axis of the cylinder, which was always mounted normal to the freestream. Both horizontal and vertical orientations were tested; gravity does not play a role in the observed phenomenon. Further details of the experiment can be found in Ref. 5. Figure 2 compares

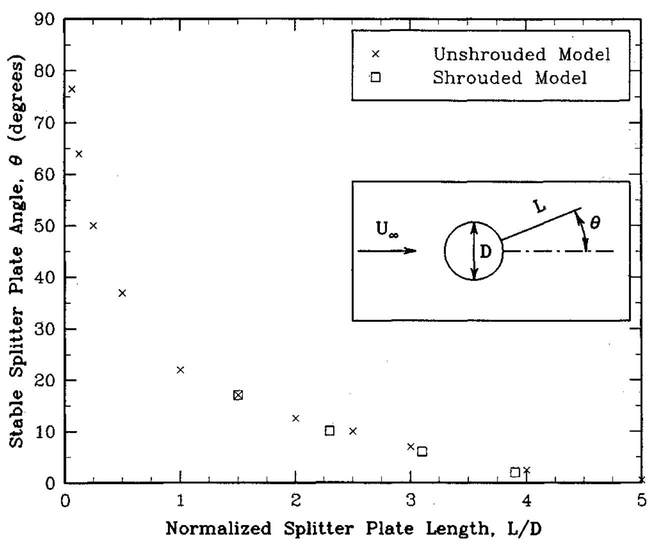

Fig. 1 Variation of stable splitter plate angle with splitter plate length for a freely rotatable cylinder/splitter plate body at Reynolds numbers between 5×10^3 and 2×10^4.

Received May 14, 1990; revision received June 13, 1990; accepted for publication June 13, 1990.

*Associate Professor, Department of Mechanical Engineering. Member AIAA.

†Graduate Assistant, Department of Mechanical Engineering.

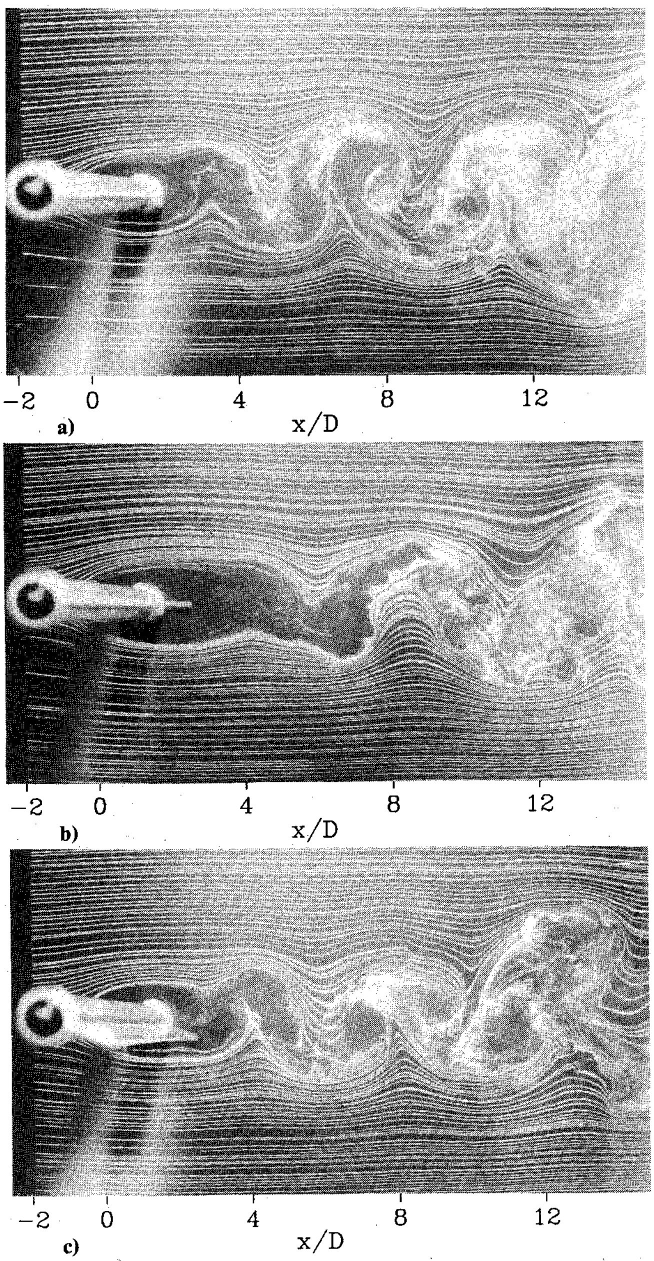

Fig. 2 Smoke-wire photographs at Re = 7.5 × 10³: a) Plain cylinder with no splitter plate, b) L/D = 1 splitter plate fixed at θ = 0 deg, c) L/D = 1 freely rotatable splitter plate.

smoke-wire flow visualizations for three cases: a) a plane cylinder, b) a cylinder with a splitter plate 1 diameter long and fixed parallel to the freestream direction, and c) the same cylinder/splitter plate body when free to rotate. Notice the position of the plate in Fig. 2c. It has rotated to its stable angle of approximately 22 deg. We will now concentrate on the near wake region.

Figures 2 reveal that the wake of the freely rotatable cylinder/splitter plate body is not grossly different from that of the plain cylinder. When fixed at 0 deg, however, the splitter plate significantly alters the wake. Specifically, the fixed splitter plate forces a delay in formation of the Karman vortex street.

For splitter plates longer than about two cylinder diameters, the wakes of the fixed and freely rotatable splitter plate bodies are nearly the same. An example is shown in Figs. 3 for the case L/D = 3. In Figs. 3a and 3b, formation of the Karman vortex street is delayed significantly.

Gerrard[6] suggested that the frequency of the Karman vortex street is inversely proportional to the length scale of the vortex formation region immediately downstream of the body. He

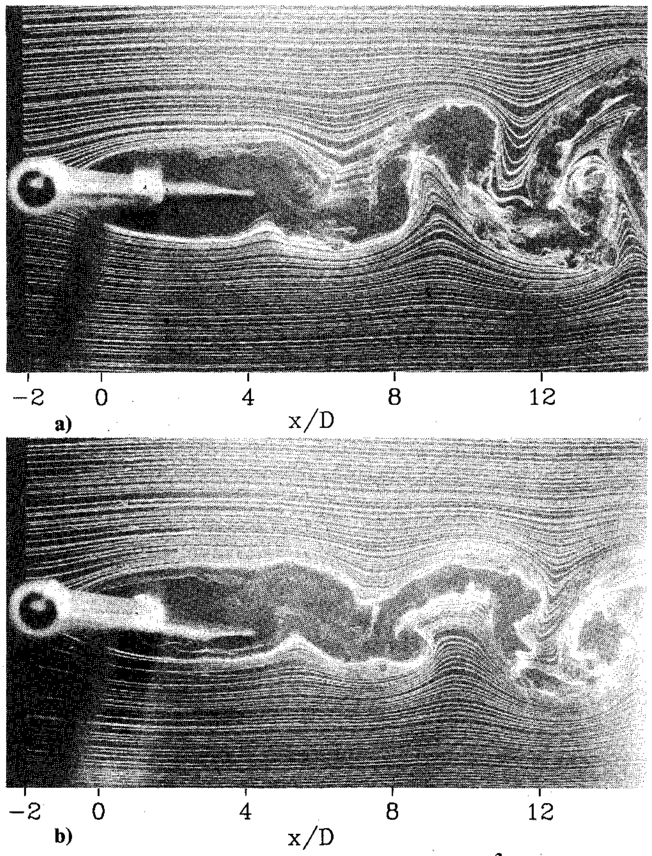

Fig. 3 Smoke-wire photographs at Re = 7.5 × 10³ and L/D = 3: a) Splitter plate fixed at θ = 0 deg, b) freely rotatable splitter plate.

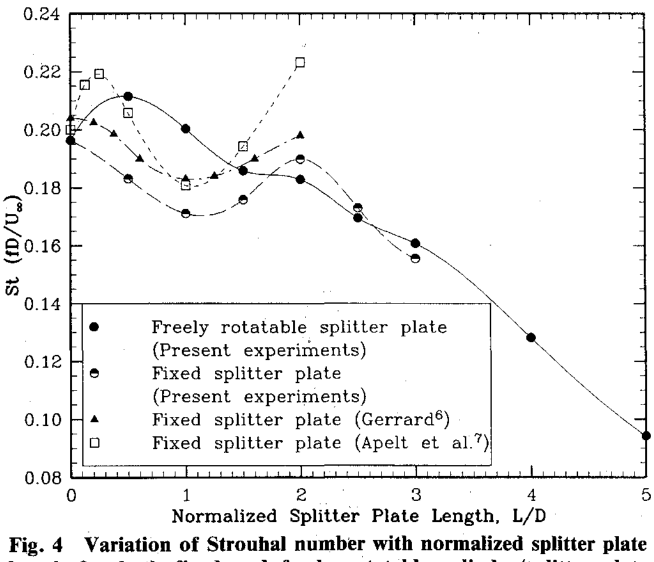

Fig. 4 Variation of Strouhal number with normalized splitter plate length for both fixed and freely rotatable cylinder/splitter plate bodies.

verified this suggestion for the case of a splitter plate forced to remain aligned with the flow. Further measurements by Bearman[2] supported Gerrard's explanation. In the present experiments, vortex shedding frequency was measured with a hot wire. Figure 4 shows the variation of Strouhal number ($St = fD/U_\infty$, where f is the vortex shedding frequency, D the cylinder diameter and U_∞ the freestream velocity) with L/D for both fixed and freely rotatable splitter plates. Also included are data for fixed plates from two earlier investigations.[6,7] It can be seen that the freely rotatable plates do not exhibit the fall and rise in St characteristic of fixed plates; rather, after a small initial increase, shedding frequency progressively decreases as plate length is increased. Gerrard's[6] explanation of vortex shedding frequency apparently applies to the freely rotatable splitter plate case as well. Namely, as the flow visualizations indicate, the vortex formation length scale increases with L/D and, hence, shedding frequency decreases with L/D. As with the flow visualizations of Fig. 3, for $L/D > 2$, the fixed and freely rotatable splitter plates behave similarly, as indicated by the overlap of data in Fig. 4.

Conclusions

When allowed to rotate freely, a splitter plate shorter than five cylinder diameters does not align itself with the freestream. Instead, it migrates to a stable position on one side of the wake or the other, with the splitter plate angle a strong function of splitter plate length, but independent of Reynolds number in the range tested. The wake of a freely rotatable splitter plate smaller than about two cylinder diameters is not significantly altered by the presence of the plate. When comparing vortex formation length and Karman vortex street shedding frequency in the near wake, a cylinder with a free splitter plate behaves much differently than does a cylinder with a rigidly mounted splitter plate of the same length. On the other hand, a freely rotatable splitter plate larger than about two cylinder diameters, although positioning itself at a nonzero angle, affects the wake in nearly the same manner as does a rigid plate of the same length. The inverse relationship between vortex formation length and vortex shedding frequency, first suggested by Gerrard,[6] is apparently valid for both fixed and free splitter plates.

References

[1]Roshko, A., "On the Development of Turbulent Wakes from Vortex Streets," NACA TN 2913, March 1953.

[2]Bearman, P. W., "Investigation of the Flow Behind a Two-Dimensional Model with a Blunt Trailing Edge and Fitted with Splitter Plates," *Journal of Fluid Mechanics*, Vol. 21, Part 2, Feb. 1965, pp. 241–255.

[3]Cimbala, J. M., Garg, S., and Park, W. J., "The Effect of a Non-Rigidly Mounted Splitter Plate on the Flow over a Circular Cylinder," *Bulletin of the American Physics Society*, Vol. 33, No. 10, Nov. 1988, p. 2249.

[4]Xu, J. C., Sen, M., and Gad-el-Hak, M., "Low-Reynolds Number Flow Over a Rotatable Cylinder-Splitter Plate Body," *Physics of Fluids A*, Vol. 2, No. 11, 1990, pp. 1925–1927.

[5]Garg, S., "An Experimental Investigation of the Effects of Non-Rigidly-Mounted Splitter Plates on the Wakes of Circular Cylinders," M.S. Thesis, Pennsylvania State University, University Park, PA, May 1990.

[6]Gerrard, J. H. "The Mechanics of the Formation Region of Vortices Behind Bluff Bodies," *Journal of Fluid Mechanics*, Vol. 25, Part 2, June, 1966, pp. 401–413.

[7]Apelt, C. J., West, G. S. and Szewczyk, A. A., "The Effects of Wake Splitter Plates on the Flow Past a Circular Cylinder in the Range $10^4 < R < 5 \times 10^4$," *Journal of Fluid Mechanics*, Vol. 61, Part 1, Oct. 1973, pp. 187–198.

Solver for Unfactored Implicit Schemes

Marcello Vitaletti*

IBM European Center for Scientific and Engineering Computing, Rome, Italy

Introduction

CODES based on implicit schemes for Euler and Navier-Stokes computations of transonic flows are very demanding in terms of computing time and storage, because the flowfield must be expressed at each time step as the solution of a large system of nonlinear equations.

The linearization of an implicit time-stepping scheme for solving the flow equations produces a system of linear equations whose coefficients matrix, hereafter referred to as the "implicit-step operator," has a sparse structure. In alternating direction implicit (ADI) schemes[1] this matrix operator is approximately factored as the product of block-tridiagonal matrices, in order to maintain the computational costs of a direct numerical-solving procedure within acceptable limits. However, the ADI factorization error prevents the use of large time steps as a method for producing a fast elimination of the transient solution in steady-state computations,[2] and it may be the main source of inaccuracy in the simulation of unsteady flows. This paper illustrates the use of the conjugate gradient squared (CGS) iterative algorithm[3] for solving the implicit-step operator in unfactored form. In the present work the flow equations are linearized at each time step, following the Beam-Warming approach, and the ADI splitting of the implicit-step operator is used to build an efficient preconditioner of the unfactored system.

Numerical Scheme

In general curvilinear coordinates, in two space dimensions, the Euler equations, describing the flow of an inviscid gas in thermodynamic equilibrium, may be written in the following strong conservation law form:

$$\partial_t \boldsymbol{q} + \partial_\xi \boldsymbol{F} + \partial_\eta \boldsymbol{G} = 0 \tag{1}$$

where $\xi = \xi(x,y,t)$ and $\eta = \eta(x,y,t)$ are the body-fitted curvilinear coordinates, and $\boldsymbol{q}$ is a vector whose four components are proportional to the conserved physical quantities of the flow. The flux vectors $\boldsymbol{F}$ and $\boldsymbol{G}$ are nonlinear functions of the flow variables $\boldsymbol{q}$ and also depend on geometric terms related to the mapping between the Cartesian and the curvilinear coordinates.[2]

By use of the Euler first-order implicit time-differencing scheme, the solution incremental change $\Delta \boldsymbol{q}^n = (\boldsymbol{q}^{n+1} - \boldsymbol{q}^\eta)$ at time $n\Delta t[\boldsymbol{q}^n = \boldsymbol{q}(n\Delta t)]$ is written as a funciton of the nonlinear flux vectors at time $(n+1)\Delta t$. A system of linear algebraic equations is then obtained by a linear expansion of the flux vectors $\boldsymbol{F}^{n+1}$ and $\boldsymbol{G}^{n+1}$ about the solution vector $\boldsymbol{q}^n$ and by a spatial discretization of the linearized probability density errors. On a numerical grid with uniform grid spacings $\Delta\xi = 1$ and $\Delta\eta = 1$, the partial derivatives are approximated by second-order centered finite-difference operators δ_ξ and δ_η such the $\delta_\xi f_{i,j} = (f_{i+1,j} - f_{i-1,j})/2$ and $\delta_\eta f_{i,j} = (f_{i,j+1} - f_{i,j+1})/2$, and the nonlinear artificial dissipation method developed by Jameson et al.[4] is used for damping high-frequency spurious oscillation modes triggered by discontinuities in the flow solution. The resulting linear algebraic system then takes the following form:

$$\{1 + \Delta t[\delta_\xi \boldsymbol{A}^n + \tilde{\delta}_\xi^2 + \tilde{\delta}_\xi^4) + (\delta_\eta \boldsymbol{B}^n + \tilde{\delta}_\eta^2 + \tilde{\delta}_\xi^4) +]\}\Delta \boldsymbol{q}^n$$

$$= -\Delta t[(\delta_\xi \boldsymbol{F}^n + \tilde{\delta}_\xi^2 \boldsymbol{q}^n + \tilde{\delta}_\xi^4 \boldsymbol{q}^n) + (\delta_\eta \boldsymbol{G}^n + \tilde{\delta}_\eta^2 \boldsymbol{q}^n + \tilde{\delta}_\eta^4 \boldsymbol{q}^n)] \tag{2}$$

where $\boldsymbol{A}^n = \partial \boldsymbol{F}(\boldsymbol{q}^n)/\partial \boldsymbol{q}$ and $\boldsymbol{B}^n = \partial \boldsymbol{G}(\boldsymbol{q}^n)/\partial \boldsymbol{q}$ are the Jacobians of the flux vectors. The three-point second-order terms $\tilde{\delta}^2 \boldsymbol{q}$ and the five-point fourth-order terms $\tilde{\delta}^2 \boldsymbol{q}$, appearing on both the implicit and the explicit side of the equations, are the artificial dissipation corrections.

The convergence of the time-marching scheme to a steady-state solution is accelerated by using a spatially varying time step $\Delta t_{i,j} = \Delta t_0/(1 + \sqrt{J_{i,j}})$, where $J_{i,j}$ is an estimate of the cell surface and the constant value Δt_0 is usually chosen in the interval between 1 and 10 for typical inviscid simulations.

Received Jan. 8, 1990; revision received June 5, 1990; accepted for publication June 26, 1990.

*Research Scientist, Via Giorgione, 159 I-00147.